Measurement of the decay B^{0}→π^{-}ℓ^{+}ν and determination of |V_{ub}|

H. Ha *et al.* (The Belle Collaboration)

Phys. Rev. D **83**, 071101 — Published 1 April 2011

DOI: 10.1103/PhysRevD.83.071101

Measurement of the decay $B^0 \to \pi^- \ell^+ \nu$ and determination of $|V_{ub}|$

H. Ha,[20] E. Won,[20] I. Adachi,[8] H. Aihara,[48] T. Aziz,[43] A. M. Bakich,[42] V. Balagura,[15] E. Barberio,[26] A. Bay,[22] K. Belous,[14] V. Bhardwaj,[38] B. Bhuyan,[11] M. Bischofberger,[28] A. Bondar,[1,36] A. Bozek,[32] M. Bračko,[24,16] T. E. Browder,[7] Y. Chao,[31] A. Chen,[29] P. Chen,[31] B. G. Cheon,[6] C.-C. Chiang,[31] I.-S. Cho,[53] K. Cho,[19] K.-S. Choi,[53] Y. Choi,[41] J. Dalseno,[25,44] M. Danilov,[15] Z. Doležal,[2] A. Drutskoy,[3] W. Dungel,[13] S. Eidelman,[1,36] N. Gabyshev,[1,36] B. Golob,[23,16] J. Haba,[8] K. Hayasaka,[27] H. Hayashii,[28] Y. Horii,[47] Y. Hoshi,[46] W.-S. Hou,[31] Y. B. Hsiung,[31] H. J. Hyun,[21] T. Iijima,[27] K. Inami,[27] R. Itoh,[8] M. Iwabuchi,[53] Y. Iwasaki,[8] N. J. Joshi,[43] T. Julius,[26] J. H. Kang,[53] T. Kawasaki,[34] C. Kiesling,[25] H. J. Kim,[21] H. O. Kim,[21] M. J. Kim,[21] S. K. Kim,[40] Y. J. Kim,[5] K. Kinoshita,[3] B. R. Ko,[20] S. Korpar,[24,16] P. Križan,[23,16] T. Kuhr,[18] T. Kumita,[49] A. Kuzmin,[1,36] Y.-J. Kwon,[53] S.-H. Kyeong,[53] J. S. Lange,[4] M. J. Lee,[40] S.-H. Lee,[20] Y. Li,[51] A. Limosani,[26] C. Liu,[39] Y. Liu,[31] D. Liventsev,[15] R. Louvot,[22] S. McOnie,[42] K. Miyabayashi,[28] H. Miyata,[34] Y. Miyazaki,[27] G. B. Mohanty,[43] T. Mori,[27] Y. Nagasaka,[9] E. Nakano,[37] M. Nakao,[8] H. Nakazawa,[29] Z. Natkaniec,[32] S. Neubauer,[18] S. Nishida,[8] K. Nishimura,[7] O. Nitoh,[50] T. Nozaki,[8] S. Ogawa,[45] T. Ohshima,[27] S. Okuno,[17] S. L. Olsen,[40,7] P. Pakhlov,[15] G. Pakhlova,[15] C. W. Park,[41] H. Park,[21] H. K. Park,[21] R. Pestotnik,[16] M. Petrič,[16] L. E. Piilonen,[51] M. Röhrken,[18] S. Ryu,[40] H. Sahoo,[7] Y. Sakai,[8] O. Schneider,[22] C. Schwanda,[13] A. J. Schwartz,[3] K. Senyo,[27] M. E. Sevior,[26] M. Shapkin,[14] C. P. Shen,[7] J.-G. Shiu,[31] F. Simon,[25,44] P. Smerkol,[16] Y.-S. Sohn,[53] A. Sokolov,[14] S. Stanič,[35] M. Starič,[16] T. Sumiyoshi,[49] Y. Teramoto,[37] K. Trabelsi,[8] S. Uehara,[8] T. Uglov,[15] Y. Unno,[6] S. Uno,[8] S. E. Vahsen,[7] G. Varner,[7] K. E. Varvell,[42] A. Vossen,[10] C. H. Wang,[30] M.-Z. Wang,[31] P. Wang,[12] M. Watanabe,[34] Y. Watanabe,[17] Y. Yamashita,[33] Z. P. Zhang,[39] P. Zhou,[52] V. Zhulanov,[1,36] T. Zivko,[16] and A. Zupanc[18]

(The Belle Collaboration)

[1]*Budker Institute of Nuclear Physics, Novosibirsk*
[2]*Faculty of Mathematics and Physics, Charles University, Prague*
[3]*University of Cincinnati, Cincinnati, Ohio 45221*
[4]*Justus-Liebig-Universität Gießen, Gießen*
[5]*The Graduate University for Advanced Studies, Hayama*
[6]*Hanyang University, Seoul*
[7]*University of Hawaii, Honolulu, Hawaii 96822*
[8]*High Energy Accelerator Research Organization (KEK), Tsukuba*
[9]*Hiroshima Institute of Technology, Hiroshima*
[10]*University of Illinois at Urbana-Champaign, Urbana, Illinois 61801*
[11]*Indian Institute of Technology Guwahati, Guwahati*
[12]*Institute of High Energy Physics, Chinese Academy of Sciences, Beijing*
[13]*Institute of High Energy Physics, Vienna*
[14]*Institute of High Energy Physics, Protvino*
[15]*Institute for Theoretical and Experimental Physics, Moscow*
[16]*J. Stefan Institute, Ljubljana*
[17]*Kanagawa University, Yokohama*
[18]*Institut für Experimentelle Kernphysik, Karlsruher Institut für Technologie, Karlsruhe*
[19]*Korea Institute of Science and Technology Information, Daejeon*
[20]*Korea University, Seoul*
[21]*Kyungpook National University, Taegu*
[22]*École Polytechnique Fédérale de Lausanne (EPFL), Lausanne*
[23]*Faculty of Mathematics and Physics, University of Ljubljana, Ljubljana*
[24]*University of Maribor, Maribor*
[25]*Max-Planck-Institut für Physik, München*
[26]*University of Melbourne, School of Physics, Victoria 3010*
[27]*Nagoya University, Nagoya*
[28]*Nara Women's University, Nara*
[29]*National Central University, Chung-li*
[30]*National United University, Miao Li*
[31]*Department of Physics, National Taiwan University, Taipei*
[32]*H. Niewodniczanski Institute of Nuclear Physics, Krakow*
[33]*Nippon Dental University, Niigata*
[34]*Niigata University, Niigata*

[35]*University of Nova Gorica, Nova Gorica*
[36]*Novosibirsk State University, Novosibirsk*
[37]*Osaka City University, Osaka*
[38]*Panjab University, Chandigarh*
[39]*University of Science and Technology of China, Hefei*
[40]*Seoul National University, Seoul*
[41]*Sungkyunkwan University, Suwon*
[42]*School of Physics, University of Sydney, NSW 2006*
[43]*Tata Institute of Fundamental Research, Mumbai*
[44]*Excellence Cluster Universe, Technische Universität München, Garching*
[45]*Toho University, Funabashi*
[46]*Tohoku Gakuin University, Tagajo*
[47]*Tohoku University, Sendai*
[48]*Department of Physics, University of Tokyo, Tokyo*
[49]*Tokyo Metropolitan University, Tokyo*
[50]*Tokyo University of Agriculture and Technology, Tokyo*
[51]*CNP, Virginia Polytechnic Institute and State University, Blacksburg, Virginia 24061*
[52]*Wayne State University, Detroit, Michigan 48202*
[53]*Yonsei University, Seoul*

We present a measurement of the charmless semileptonic decay $B^0 \to \pi^- \ell^+ \nu$ using a data sample containing 657×10^6 $B\bar{B}$ events collected with the Belle detector at the KEKB asymmetric-energy e^+e^- collider operating near the $\Upsilon(4S)$ resonance. We determine the total branching fraction of the decay, $\mathcal{B}(B^0 \to \pi^- \ell^+ \nu) = (1.49 \pm 0.04(\text{stat}) \pm 0.07(\text{syst})) \times 10^{-4}$. We also report a new precise measurement of the differential decay rate, and extract the Cabibbo-Kobayashi-Maskawa matrix element $|V_{ub}|$ using model-independent and model-dependent approaches. From a simultaneous fit to the measured differential decay rate and lattice QCD results, we obtain $|V_{ub}| = (3.43 \pm 0.33) \times 10^{-3}$, where the error includes both experimental and theoretical uncertainties.

PACS numbers: 12.15.Hh, 13.20.He, 12.38.Qk

Weak transitions among quark flavors in the standard model (SM) are described by the Cabibbo-Kobayashi-Maskawa (CKM) matrix [1], in which $|V_{ub}|$ is one of the least known elements. Precise measurements of the values of the CKM matrix elements are necessary to probe the quark mixing mechanism of the SM and to search for possible physics beyond the SM. The magnitude of the CKM element V_{ub} can be determined from exclusive $b \to u\ell\nu$ semileptonic decays, of which $B^0 \to \pi^- \ell^+ \nu$ [2] yields the most precise value for $|V_{ub}|$. The differential rate of this decay can be expressed in terms of $|V_{ub}|$ and the form factor $f_+(q^2)$, where q^2 is the square of the momentum transferred from the B meson to the outgoing leptons, $q^2 = (p_\ell + p_\nu)^2$ [3]. The present theoretical understanding of $f_+(q^2)$ is limited, which is a significant source for systematic uncertainty in the extraction of $|V_{ub}|$ from this decay. Predictions have been obtained in unquenched lattice QCD [4, 5], in light cone sum rule (LCSR) theory [6] and in relativistic quark models [7]. However, these predictions typically assume a specific shape for $f_+(q^2)$ and provide reliable predictions only in a limited q^2 range (lattice QCD is valid near q^2 maximum, while LCSR is reliable near the minimum value of q^2). Recently, it has been shown that a determination of $|V_{ub}|$ independent of a form factor shape calculation can be achieved by simultaneously fitting the measured q^2 spectrum and lattice QCD results computed near the zero recoil of q^2 range [8, 9], resulting in $|V_{ub}| = (3.38 \pm 0.36) \times 10^{-3}$ using the experimental data in Ref. [10] for the decay $B^0 \to \pi^- \ell^+ \nu$ where the error includes both theoretical and experimental uncertainties. The experimental uncertainty is a 6% while the theoretical contribution is estimated to be an 8.5% [9]. In addition, Ref. [11] reports $|V_{ub}| = (2.95 \pm 0.31) \times 10^{-3}$ by combining measurements of $B^0 \to \pi^- \ell^+ \nu$ and $B^+ \to \pi^0 \ell^+ \nu$; here the error contains a 3% contribution from the branching fraction measurement, a 5% from the shape of the q^2 spectrum measured in data, and an 8.5% from the theoretical normalization. Here we describe a study of the decay $B^0 \to \pi^- \ell^+ \nu$ and measure the branching fraction and the q^2 spectrum. We then compare with other recent studies of this decay [10–15]. The differential branching fraction is measured in 13 bins of q^2, and $|V_{ub}|$ is determined using both model-independent and model-dependent approaches.

The Belle detector [16, 17] is a large-solid-angle magnetic spectrometer that consists of a silicon vertex detector (SVD), a 50-layer central drift chamber (CDC), an array of aerogel threshold Cherenkov counters (ACC), a barrel-like arrangement of time-of-flight scintillation counters (TOF), and an electromagnetic calorimeter composed of CsI(Tl) crystals (ECL) located inside a superconducting solenoid coil that provides a 1.5 T magnetic field. An iron flux-return located outside of the coil is instrumented with resistive plate chambers to detect K_L^0 mesons and to identify muons (KLM).

The data sample corresponds to an integrated luminosity of 605 fb^{-1} taken at a center-of-mass (c.m.) energy near the $\Upsilon(4S)$ resonance, containing 657×10^6 $B\bar{B}$ pairs. For the first sample of 152×10^6 $B\bar{B}$ events, an inner detector configuration with a 2.0 cm beampipe and a 3-layer SVD was used, while a 1.5 cm beampipe, a 4-layer SVD and a small-cell inner drift chamber were used to record the remaining 505×10^6 $B\bar{B}$ pairs [18]. Another 68 fb^{-1} data sample taken at a c.m. energy 60 MeV below the resonance is used to study the continuum background, $e^+e^- \rightarrow q\bar{q}$, where $q = u, d, s, c$. Monte Carlo (MC) [19, 20] simulated events equivalent to at least ten times the integrated luminosity were generated to model the signal. Samples equivalent to ten times and six times the integrated luminosity were generated to simulate the two largest background components, $b \rightarrow c$ decays and continuum, respectively. To simulate rare $b \rightarrow u$ decays, samples equivalent to twenty times the integrated luminosity were generated. Final state radiation (FSR) from charged particles in the final state is modeled using the PHOTOS package [21].

The decay $B^0 \rightarrow \pi^-\ell^+\nu$ is reconstructed from pairs of oppositely charged leptons and pions. Electron candidates are identified using the ratio of the energy detected in the ECL to the track momentum, the ECL shower shape, position matching between the track and ECL cluster, the energy loss in the CDC, and the response of the ACC counters [22]. Bremsstrahlung photons emitted close to the electron direction are reconstructed and used to correct the electron momentum [23]. Muons are identified based on their penetration range and transverse scattering in the KLM detector [24]. In the momentum region relevant to this analysis, charged leptons are identified with an efficiency of about 90% while the probability to misidentify a pion as an electron (muon) is 0.25% (1.4%). Pion candidates are selected with an efficiency of 85% and a kaon misidentification probability of 19%, based on the responses of the CDC, ACC and TOF subdetectors. All charged particles are required to originate from the interaction point (IP) and to have associated hits in the SVD. The pion and lepton candidates are fitted to a common vertex and the confidence level of the fit is required to be greater than 1.0%. The electron (muon) is required to have a laboratory frame momentum greater than 0.8 GeV/c (1.1 GeV/c).

The missing energy and momentum in the c.m. frame are defined as $E_{\rm miss} \equiv 2E_{\rm beam} - \sum_i E_i$ and $\vec{p}_{\rm miss} \equiv -\sum_i \vec{p}_i$, respectively, where $E_{\rm beam}$ is the beam energy in the c.m. frame, and the sums include all charged and neutral particle candidates in the event. A threshold energy of 50 (100) MeV is required for photon candidates in the central (side) region of the ECL. The neutrino 4-momentum is taken to be $p_\nu = (|\vec{p}_{\rm miss}|,\ \vec{p}_{\rm miss})$, since the determination of $\vec{p}_{\rm miss}$ is more accurate than that of the missing energy. To select events compatible with the signal decay mode, we require $|Q_{\rm total}| \leq 3$, where $Q_{\rm total}$ is the net charge of the event, and $E_{\rm miss} > 0$ GeV. We denote the combined system of the signal pion and lepton as Y. The kinematics of the decay constrain the cosine of the angle between the B and Y directions in the c.m. frame, defined by $\cos\theta_{BY} = (2E_{\rm beam}E_Y - m_B^2 - M_Y^2)/(2|\vec{p}_B||\vec{p}_Y|)$, where m_B and $|p_B| = \sqrt{E_{\rm beam}^2 - m_B^2}$ refer to the mass and momentum of the B meson, and E_Y, M_Y, and p_Y refer to the energy, mass, and momentum of the reconstructed Y. Background, on the other hand, is not similarly constrained. In what follows we require $|\cos\theta_{BY}| \leq 1$. Signal candidates are classified by their beam-energy-constrained mass, $M_{\rm bc} = \sqrt{E_{\rm beam}^2 - |\vec{p}_\pi + \vec{p}_\ell + \vec{p}_\nu|^2}$, and energy difference, $\Delta E = E_{\rm beam} - (E_\pi + E_\ell + E_\nu)$. Candidates outside of the signal region, defined by the requirements $M_{\rm bc} > 5.19$ GeV/c^2 and $|\Delta E| < 1$ GeV, are rejected. To suppress background from the continuum, the ratio of second to zeroth Fox-Wolfram moments [25] is required to be less than 0.35. Background from $J/\psi \rightarrow \mu^+\mu^-$ decays with one muon misidentified as a pion is rejected by vetoing events with a Y mass between 3.07 GeV/c^2 and 3.13 GeV/c^2. The sample of signal candidates is divided into 13 bins of q^2 from 0 to 26.4 GeV^2/c^2 (the bin width is 2 GeV^2/c^2, except for the last bin). The value of q^2 is calculated as the square of the difference between the 4-momenta of the B meson and that of the pion. As the B direction is only kinematically constrained to lie on a cone around the Y direction, we take a weighted average over four different possible configurations of the B direction [26]. Background is fur-

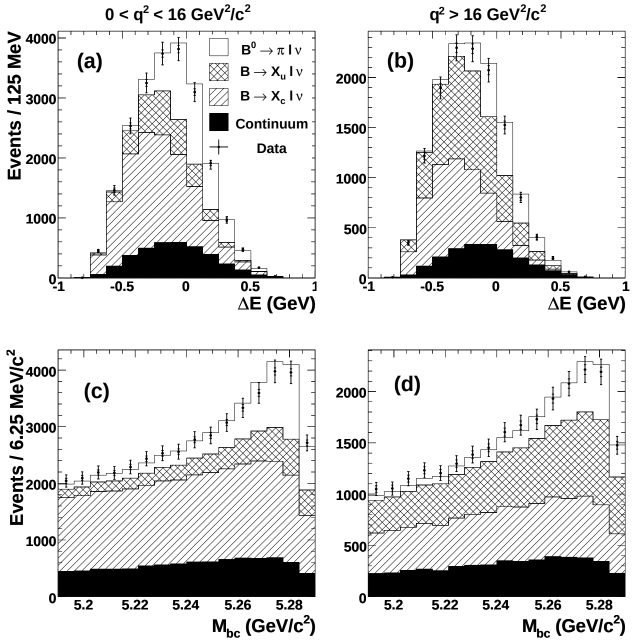

FIG. 1: Fit projections (a,b) in ΔE with $M_{\rm bc} > 5.27$ GeV/c^2, and (c, d) in $M_{\rm bc}$ with $|\Delta E| < 0.125$ GeV. The projections (a,c) and (b,d) show the regions $q^2 < 16$ GeV^2/c^2 and $q^2 > 16$ GeV^2/c^2, respectively. The points with error bars are $\Upsilon(4S)$ data, the histograms are (from top to bottom) $B^0 \rightarrow \pi^-\ell^+\nu$ signal (open), $B \rightarrow X_u\ell\nu$ (cross-hatched), $B \rightarrow X_c\ell\nu$ (hatched) and continuum background (black-filled). The smaller error bars are statistical only while the larger ones include systematic uncertainties.

ther suppressed by applying selection criteria as a function of q^2 to the following quantities: the angle between the thrust axis of the Y system and the thrust axis of the rest of the event; the angle of the missing momentum with respect to the beam axis; the helicity angle of the $\ell\nu$ system [27]; and the missing mass squared of the event, $M^2_{\rm miss} = E^2_{\rm miss} - \vec{p}^{\,2}_{\rm miss}$. The helicity angle is the angle between the lepton direction and the direction opposite to the B meson in the $\ell\nu$ rest frame. These selections are optimized separately in each bin of q^2 by maximizing the figure-of-merit $S/\sqrt{(S+B)}$, where S (B) is the expected number of signal (background) events.

The fraction of events that have multiple candidates is 66%. To remove multiple signal candidates in a single event, the candidate with the smallest $\ell\nu$ helicity angle is selected. After imposing all selections described above, the reconstruction efficiency for signal ranges from 7.7% to 15.0% over the entire q^2 range. The fraction of the self-cross-feed component, in which one or more of the signal tracks are not correctly reconstructed, is 3.5%.

The signal yield is determined by performing a two-dimensional, binned maximum likelihood fit to the $(M_{\rm bc}, \Delta E)$ plane in 13 bins of q^2 [28]. Background contributions from $b \to u\ell\nu$, $b \to c\ell\nu$ and non-$B\bar{B}$ continuum are considered in the fit. Probability density functions (PDFs) corresponding to these fit components are obtained from MC simulations. To reduce the number of free parameters, the q^2 bins of the background components are grouped into coarser bins: four bins for $b \to u\ell\nu$, and three bins for $b \to c\ell\nu$. The choice of the binning was chosen from the total statistical error, number of parameters to fit, and the complexity of the fits. The q^2 distribution of the continuum MC [29] simulation is reweighted to match the corresponding distribution in off-resonance data. For this procedure, a continuum MC sample about 60 times the integrated luminosity of the off-resonance data is used. The continuum normalization is fixed to the scaled number of off-resonance events, 52928 events. Including signal yields in each q^2 bin, there are 20 free parameters in the fit.

We obtain 21486 ± 548 signal events, 52543 ± 1148 $b \to u\ell\nu$ events, and 161829 ± 976 $b \to c\ell\nu$ background events. These yields agree well with the expectations from MC simulation studies. The χ^2/n.d.f. of the fit is 2962/3308. The projections of the fit result in ΔE and $M_{\rm bc}$ are shown in Fig. 1 for the regions $q^2 < 16$ GeV$^2/c^2$ and $q^2 > 16$ GeV$^2/c^2$. Bin-to-bin migrations due to q^2 resolution are corrected by applying the inverse detector response matrix [30] to the measured partial yields. The partial branching fractions $\Delta\mathcal{B}$ are calculated using the signal efficiencies obtained from MC simulation. The total branching fraction $\mathcal{B}$ is the sum of partial branching fractions taking into account correlations when calculating the errors. We find $\mathcal{B}(B^0 \to \pi^-\ell^+\nu) = (1.49 \pm 0.04({\rm stat}) \pm 0.07({\rm syst})) \times 10^{-4}$, where the first error is statistical and the second error is systematic. This result is significantly more precise than our previous measurement [13] with $B \to D^{(*)}\ell^+\nu$ tags on a 253 fb^{-1} data sample.

To estimate the systematic uncertainties on $\Delta\mathcal{B}$, we include the following contributions: the uncertainties in lepton and pion identification, the charged particle reconstruction, the photon detection efficiency, and the requirement on the χ^2 probability of the vertex fit, which is estimated by comparing results with and without this requirement. The results are summarized as detector effects in Table I. They depend weakly on q^2 and amount to 3.4% for the entire q^2 range. We vary the branching fractions of the decays contributing to the $b \to u\ell\nu$ and $b \to c\ell\nu$ backgrounds within ±1 standard deviation of their world-average values [31] and assign an uncertainty of 0.6% to the total yield. We further consider form factor uncertainties in the decays $B^0 \to \pi^-\ell^+\nu$ [14], $B^0 \to \rho^-\ell^+\nu$ [6, 32], $B^0 \to D^-\ell^+\nu$ and $B^0 \to D^{*-}\ell^+\nu$ [33], and uncertainties in the shape function parameters of the inclusive $b \to u\ell\nu$ model [34]. These uncertainties correspond to a 1.1% error on $\mathcal{B}(B^0 \to \pi^-\ell^+\nu)$. The uncertainty in the correction of the continuum MC is estimated by varying its weights by their statistical uncertainties. The other sources of systematic uncertainty in Table I include the uncertainty in the $\Upsilon(4S) \to B^0\bar{B}^0$ branching fraction [31], limited MC statistics, the effect of final state radiation, which is estimated by investigating MC samples with and without bremsstrahlung corrections calculated using the PHOTOS package, and the uncertainty in the number of $B\bar{B}$ pairs in the data sample. For values of $\Delta\mathcal{B}$ in individual q^2 bins, a break-

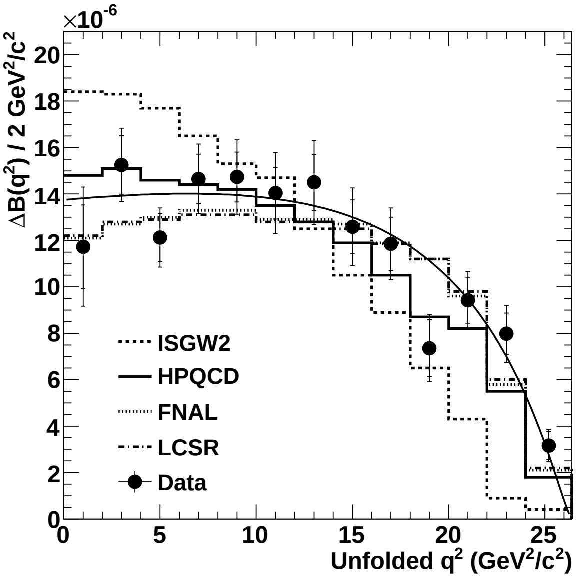

FIG. 2: Distribution of the partial branching fraction as a function of q^2 after unfolding (closed circles). The error bars show the statistical and the total uncertainty on the data. The curve is the result of a fit of the BK form factor parameterization [36] to our data. The four histograms (dashed:ISGW2; plain:HPQCD; dotted:FNAL; dot-dashed:LCSR) show various form factor predictions.

TABLE I: Values of $\Delta\mathcal{B}(q^2)$ and relative uncertainties (%). The uncertainties in MC input parameters are given separately for branching fractions (BF) and form factors (FF).

$q^2(\mathrm{GeV}^2/c^2)$	0 - 6	6 - 12	12 - 18	18 - 26.4	0 - 16	16 - 26.4	Total
$\Delta\mathcal{B}$ ($\times$ 10^7)	391.19	434.25	389.47	279.18	1096.34	397.75	1494.09
Detector effects	3.4	3.5	3.5	3.5	3.4	3.5	3.4
Physics parameters (BF)	0.8	0.7	0.6	0.7	0.6	0.6	0.6
Physics parameters (FF)	1.9	1.7	1.9	1.8	1.3	1.8	1.1
Continuum correction	4.4	2.3	3.4	2.3	2.1	2.6	1.8
Other sources	2.1	2.5	2.4	2.4	2.1	2.3	2.0
Total statistical error	5.3	3.9	4.8	6.1	3.0	5.3	2.6
Total error	8.2	6.5	7.5	8.1	5.7	7.5	5.2

down of the systematic uncertainties and the statistical and systematic correlations is given in the accompanying EPAPS document [35].

We fit the $\Delta\mathcal{B}$ distribution using the two-parameter BK parameterization [36] of $f_+(q^2)$, taking into account statistical and systematic correlations. The result is shown in Fig. 2. Although this parameterization has been criticized [37], we present the fit result in order to directly compare with other existing results [10]. We obtain $|V_{ub}|f_+(0) = (9.24 \pm 0.18(\mathrm{stat}) \pm 0.21(\mathrm{syst})) \times 10^{-4}$ and $\alpha = 0.60 \pm 0.03(\mathrm{stat}) \pm 0.02(\mathrm{syst})$, where α is a positive constant that scales with m_B [36]. The χ^2 probability of the fit is 62%. We also calculate the χ^2 probabilities of different theoretical form factor predictions with our binned data. We obtain probabilities of 42% and 43% for the HPQCD [4] and the FNAL [5] lattice QCD calculations, respectively, and 49% for the LCSR theory [6]. The ISGW2 quark model [7], for which the probability is 2.3×10^{-6}, is incompatible with the experimental data.

As described in Ref. [9], the CKM matrix element $|V_{ub}|$ can be extracted from a simultaneous fit to experimental and lattice QCD results (from the FNAL/MILC Collaboration [9]), taking into account statistical and systematic correlations. To this end, the q^2 variable is transformed to a dimensionless variable z [8, 37]. In addition, the two functions, P_+ and ϕ_+ are taken from Ref. [38], where P_+ is a function that accounts for the pole at $q^2 = m^2_{B^*}$ and ϕ_+ is an analytic function that controls the values of the a_i series coefficients. In terms of the new variable z, the product of the form factor $f_+(q^2)$ and the functions P_+ and ϕ_+ has the simple form, $\sum_{i=0}^{\infty} a_i z^i$. We fit the lattice QCD results and experimental data with a third-order polynomial where the free parameters of the fit are the coefficients a_i and the relative normalization between lattice QCD results and experimental results, which is $|V_{ub}|$. The resulting experimental data (which are scaled by the fitted $|V_{ub}|$ value) and the lattice QCD results are shown in Fig. 3. We obtain $|V_{ub}| = (3.43 \pm 0.33) \times 10^{-3}$, $a_0 = 0.022 \pm 0.002$, $a_1 = -0.032 \pm 0.004$, $a_2 = -0.080 \pm 0.020$ and $a_3 = 0.081 \pm 0.066$, where the χ^2/n.d.f. of the fit is approximately 12/20. Statistically, we find no significant difference in the fitted value of $|V_{ub}|$ using second- and fourth-order polynomial fits. Note that the error in $|V_{ub}|$ includes both experimental and theoretical uncertainties. We find that the error includes a 3% contribution from the branching fraction measurement, a 4% from the q^2 shape measured in data, and an 8% uncertainty from theoretical normalization. The experimental and the total errors are compatible with the previous results in Ref. [9, 11].

Alternatively, $|V_{ub}|$ can be determined from the measured partial branching fraction using the relation $|V_{ub}| = \sqrt{\Delta\mathcal{B}/(\tau_{B^0}\Delta\zeta)}$, where τ_{B^0} is the B^0 lifetime [31] and $\Delta\zeta$ is the normalized partial decay width derived in different theoretical approaches [4–6]. These calculations typically assume a specific parameterization of the form factor shape. Values of $|V_{ub}|$ for different form factor predictions are given in Table II.

In summary, using $657{\times}10^6$ $B\bar{B}$ events of Belle $\Upsilon(4S)$ data we measure the partial branching fractions

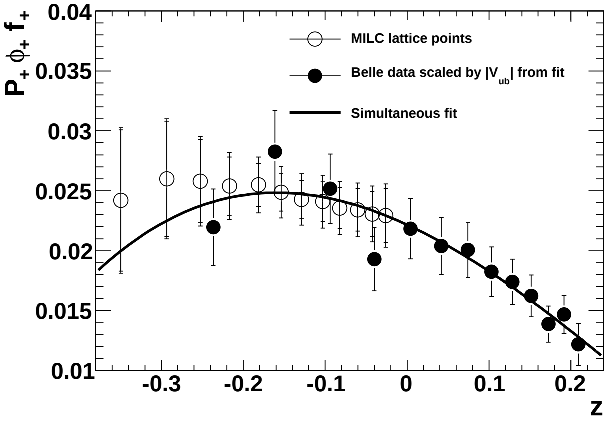

FIG. 3: $|V_{ub}|$ extraction from a simultaneous fit of experimental (closed circles) and FNAL/MILC lattice QCD results (open circles) [9]. The error for each experimental data point is the total experimental uncertainty. The smaller error bars of the lattice QCD results are statistical only while the larger ones also include systematic uncertainties.

TABLE II: Values extracted for $|V_{ub}|$ using different form factor predictions. The first error on $|V_{ub}|$ is the experimental error including statistical, systematic uncertainties and the uncertainty in the B^0 lifetime [31], the last asymmetric errors arise from the uncertainty in $\Delta\zeta$.

$f_+(q^2)$	q^2 (GeV$^2/c^2$)	$\Delta\zeta$ (ps^{-1})	$\lvert V_{ub}\rvert$ (10^{-3})
HPQCD [4]	> 16	2.07 ± 0.57	$3.55 \pm 0.13^{+0.62}_{-0.41}$
FNAL [5]	> 16	1.83 ± 0.50	$3.78 \pm 0.14^{+0.65}_{-0.43}$
LCSR [6]	< 16	5.44 ± 1.43	$3.64 \pm 0.11^{+0.60}_{-0.40}$

of the decay $B^0 \to \pi^- \ell^+ \nu$ in 13 bins of q^2. The total branching fraction is found to be $(1.49 \pm 0.04(\text{stat}) \pm 0.07(\text{syst})) \times 10^{-4}$. A combined fit of experimental and FNAL/MILC lattice QCD results [9], yields a new precise determination of $|V_{ub}|$ from this decay, $|V_{ub}| = (3.43 \pm 0.33) \times 10^{-3}$. Determinations using only a fraction of the phase space lead to less precise but statistically compatible numbers for $|V_{ub}|$: using a LCSR calculation for the region $q^2 < 16$ GeV$^2/c^2$ [6] yields $(3.64 \pm 0.06(\text{stat}) \pm 0.09(\text{syst})^{+0.60}_{-0.40}(\text{FF})) \times 10^{-3}$. Assuming the HPQCD [5] and the FNAL [4] lattice QCD calculations, sensitive to the region $q^2 > 16$ GeV$^2/c^2$, we obtain $(3.55 \pm 0.09(\text{stat}) \pm 0.09(\text{syst})^{+0.62}_{-0.41}(\text{FF})) \times 10^{-3}$ and $(3.78 \pm 0.10(\text{stat}) \pm 0.10(\text{syst})^{+0.65}_{-0.43}(\text{FF})) \times 10^{-3}$, respectively.

We thank the KEKB group for excellent operation of the accelerator, the KEK cryogenics group for efficient solenoid operations, and the KEK computer group and the NII for valuable computing and SINET3 network support. We acknowledge support from MEXT, JSPS and Nagoya's TLPRC (Japan); ARC and DIISR (Australia); NSFC (China); MSMT (Czechia); DST (India); MEST, NRF, NSDC of KISTI, and WCU (Korea); MNiSW (Poland); MES and RFAAE (Russia); ARRS (Slovenia); SNSF (Switzerland); NSC and MOE (Taiwan); and DOE (USA). E. Won acknowledges support by NRF Grant No. 2009-0071072.

---

[1] M. Kobayashi and T. Maskawa, Prog. Theor. Phys. **49**, 652 (1973); N. Cabibbo, Phys. Rev. Lett. **10**, 531 (1963).

[2] Throughout this paper, the inclusion of the charge-conjugate decay mode is implied unless otherwise stated.

[3] M. Neubert, Phys. Rept. **245**, 259 (1994).

[4] E. Dalgic, A. Gray, M. Wingate, C. T. H. Davies, G. P. Lepage and J. Shigemitsu, Phys. Rev. D **73**, 074502 (2006). [Erratum-ibid. D **75**, 119906 (2007)].

[5] M. Okamoto *et al.*, Nucl. Phys. Proc. Suppl. **140**, 461 (2005).

[6] P. Ball and R. Zwicky, Phys. Rev. D **71**, 014015 (2005).

[7] D. Scora and N. Isgur, Phys. Rev. D **52**, 2783 (1995).

[8] C. G. Boyd, B. Grinstein and R. F. Lebed, Phys. Rev. Lett. **74**, 4603 (1995); C. G. Boyd and M. J. Savage, Phys. Rev. D **56**, 303 (1997).

[9] J. A. Bailey *et al.* (Fermilab Lattice and MILC Collaboration), Phys. Rev. D **79**, 054507 (2009).

[10] B. Aubert *et al.* (BaBar Collaboration), Phys. Rev. Lett. **98**, 091801 (2007).

[11] arXiv:1005.3288v2 [hep-ex], submitted to Phys. Rev. D. P. del Amo Sanchez *et al.* (BaBar Collaboration).

[12] S. B. Athar *et al.* (CLEO Collaboration), Phys. Rev. D **68**, 072003 (2003).

[13] T. Hokuue *et al.* (Belle Collaboration), Phys. Lett. B **648**, 139 (2007).

[14] B. Aubert *et al.* (BaBar Collaboration), Phys. Rev. D **72**, 051102 (2005).

[15] B. Aubert *et al.* (BaBar Collaboration), Phys. Rev. Lett. **97**, 211801 (2006).

[16] A. Abashian *et al.*, Nucl. Instrum. Meth. A **479**, 117 (2002).

[17] S. Kurokawa, Nucl. Instrum. Meth. A **499**, 1 (2003), and other papers included in this volume.

[18] Z. Natkaniec *et al.*, Nucl. Instrum. Meth. A **560** 1, (2006).

[19] D. J. Lange, Nucl. Instrum. Meth. A **462**, 152 (2001).

[20] R. Brun *et al.*, "GEANT3.21," CERN Report No. DD/EE/84-1, 1987.

[21] E. Barberio and Z. Was, Comput. Phys. Commun. **79**, 291 (1994).

[22] K. Hanagaki, H. Kakuno, H. Ikeda, T. Iijima and T. Tsukamoto, Nucl. Instrum. Meth. A **485**, 490 (2002).

[23] C. Schwanda *et al.* (Belle Collaboration), Phys. Rev. D **75**, 032005 (2007).

[24] A. Abashian *et al.*, Nucl. Instrum. Meth. A **491**, 69 (2002).

[25] G. C. Fox and S. Wolfram, Phys. Rev. Lett. **41**, 1581 (1978).

[26] B. Aubert *et al.* (BaBar Collaboration), Phys. Rev. D **74**, 092004 (2006).

[27] D. Cote, S. Brunet, P. Taras and B. Viaud, Eur. Phys. J. C **38**, 105 (2004).

[28] R. J. Barlow and C. Beeston, Comput. Phys. Commun. **77**, 219 (1993).

[29] T. Sjostrand, Comput. Phys. Commun. **82**, 74 (1994).

[30] G. Cowan, *Statistical Data Analysis* (Oxford University, Oxford, UK, 1998), Chap. 11.

[31] C. Amsler *et al.* [Particle Data Group], Phys. Lett. B **667**, 1 (2008).

[32] P. Ball and R. Zwicky, Phys. Rev. D **71**, 014029 (2005).

[33] D. Asner *et al.* (The Heavy Flavor Averaging Group), arXiv:1010.1589v1 [hep-ex] and online update at `http://www.slac.stanford.edu/xorg/hfag/`.

[34] F. De Fazio and M. Neubert, JHEP **9906**, 017 (1999).

[35] See the EPAPS Document for tables of systematic errors and error matrices. For more information on EPAPS, see `http://www.aip.org/pubservs/epaps.html`.

[36] D. Becirevic and A. B. Kaidalov, Phys. Lett. B **478**, 417 (2000).

[37] T. Becher and R. J. Hill, Phys. Lett. B **633**, 61 (2006).

[38] M. C. Arnesen, B. Grinstein, I. Z. Rothstein, and I. W. Stewart, Phys. Rev. Lett. **95**, 071802 (2005).